




Cosmological selection of a small weak scale from large vacuum energy: a minimal approach

Susobhan Chattopadhyay ^a Dibya S. Chattopadhyay ^a Rick S. Gupta ^a

^a *Tata Institute of Fundamental Research, Homi Bhabha Road, Colaba, Mumbai 400005, India*

E-mail: susobhan.chattopadhyay@tifr.res.in,

d.s.chattopadhyay@theory.tifr.res.in, rsgupta@theory.tifr.res.in

ABSTRACT: We present a minimal cosmological solution to the hierarchy problem. Our model consists of a light pseudoscalar and an extra Higgs doublet in addition to the field content of the Standard Model. We consider a landscape of vacua with varying values of the electroweak vacuum expectation value (VEV). The vacuum energy in our model peaks in a region of the landscape where the electroweak VEV is non-zero and much smaller than the cutoff. During inflation, due to exponential expansion, such regions of the landscape with maximal vacuum energy, dominate the universe in volume, thus explaining the smallness of the electroweak scale with respect to the cutoff. The pseudoscalar potential in our model is that of a completely generic pseudogoldstone boson—not requiring the clockwork mechanism—and its field value never exceeds its decay constant or the Planck scale. Our mechanism is robust to the variation of other model parameters in the landscape along with the electroweak VEV. It also predicts a precise and falsifiable relationship between the masses and couplings of the different Higgs boson mass-eigenstates. Moreover, the pseudoscalar in our model can account for the observed dark matter relic density.

Contents

1	Introduction	1
2	A small weak scale from large vacuum energy	3
2.1	Model	3
2.2	Cosmological set-up and the landscape	5
2.3	Maximisation of vacuum energy	7
2.4	Volume of desired region	12
3	Phenomenology of the 2HDM sector	15
4	Phenomenology of ϕ and dark matter	17
4.1	Quartic regime	18
4.2	Quadratic regime and wave-like dark matter	19
5	Conclusions	21
A	Quantum Fluctuations and the volume-weighted Fokker-Planck equation	22
B	Minimization of the 2HDM potential	23

1 Introduction

The hierarchy problem has been one of the central themes of particle physics research in the last few decades. Most of the approaches to solve the hierarchy problem involve embedding the Standard Model into a larger framework where some new symmetry—such as supersymmetry or a shift symmetry—is recovered in the limit, $\mu^2 \rightarrow 0$, μ^2 being the Higgs mass squared parameter. The Higgs mass in these theories is thus related to the scale of breaking of this new symmetry which results in the prediction of new particles at the TeV scale such as superpartners or composite states. There is thus a growing tension between the predictions of these models and the lack of any evidence for new physics at the LHC.

This situation has led to the emergence of a new approach to the hierarchy problem where the, $\mu^2 = 0$, point is special—not from the point of view of symmetry—but because it separates two different phases, namely, the electroweak breaking and preserving phases. Models using this approach [1–15] propose mechanisms for the Higgs sector to spontaneously evolve to a near-critical state, making them somewhat reminiscent of systems exhibiting self-organized criticality [16, 17]. They use the electroweak vacuum expectation value (VEV) to trigger some cosmological dynamics that provides a non-anthropoc mechanism to select a small but negative Higgs mass squared from a landscape of possible values,

$-\Lambda^2 \lesssim \mu^2 \lesssim \Lambda^2$, Λ being the cutoff. This landscape can either be physically realized by a variation of μ^2 over causally disconnected patches during inflation or, as in relaxation models [3], can be scanned only in time, for instance, by a slowly rolling scalar field. Unlike the anthropic approach [18, 19], these models provide clear testable signatures.

The central idea of our work is the observation that there is already a physical quantity in the Standard Model—namely the vacuum energy contribution from the Higgs potential—that behaves in a special way at the boundary between the electroweak symmetry broken and unbroken phases (see also Ref. [6, 11]). In the unbroken phase, the vacuum energy contribution is constant and independent of the Higgs potential parameters. In the broken phase, on the other hand, it drops monotonically with the electroweak VEV as the Higgs minimum becomes deeper. We propose a model where the Standard Model (SM) Higgs sector is promoted to a two Higgs doublet model (2HDM) with an additional light pseudoscalar, ϕ . The vacuum energy of the 2HDM- ϕ system decreases for large electroweak VEVs—a feature our model inherits from the SM. Unlike the SM, however, the vacuum energy contribution peaks at a non-zero value of the electroweak VEV that is much smaller than the cutoff.

We assume a landscape of values for the parameters of the 2HDM- ϕ -potential that is realized in an eternally inflating ‘multiverse’. We then utilize the observation made by Ref. [5] (and further developed in Ref. [6, 8, 11]) that regions of the multiverse with maximal vacuum energy—that in our model also have a large hierarchy between the electroweak scale and the cutoff—will expand at an exponentially faster rate compared to other regions and will thus eventually dominate in volume. A schematic description of our mechanism has been presented in Fig. 1. A possible concern in all models that utilize the idea of Ref. [5], is the implicit use of a volume based measure for the multiverse; this can be problematic because of the so-called youngness paradox [20]. As we will show, however, with an appropriate choice of the measure, our mechanism can explain the Higgs mass hierarchy while not running into any such paradoxes.

Our model has several attractive features: (1) the ϕ -potential in our model is that of a generic light scalar, for eg. a pseudo-Nambu goldstone boson (PNGB), and does not require a clockwork-like mechanism; (2) the ϕ -field value never exceeds its ‘decay constant’, f , let alone the Planck scale; (3) unlike the anthropic argument for a weak scale [19], our mechanism does not restrict the variation of other model parameters as the electroweak VEV is varied; (4) the number of e-folds in the slow-roll phase of inflation does not need to be very large; (5) there is a precise, falsifiable prediction that analytically relates different masses and couplings of the 2HDM sector; and finally, (6) the pseudoscalar, ϕ , can account for the observed dark matter density via the misalignment mechanism.

The plan of the paper is as follows. In Sec. 2 we describe our mechanism in detail. In Sec. 3 we discuss the phenomenology of the 2HDM sector whereas in Sec. 4 we discuss the phenomenology of the ϕ -field and the possibility that it can account for the observed dark matter relic density. Finally, we make some concluding remarks in Sec. 5.

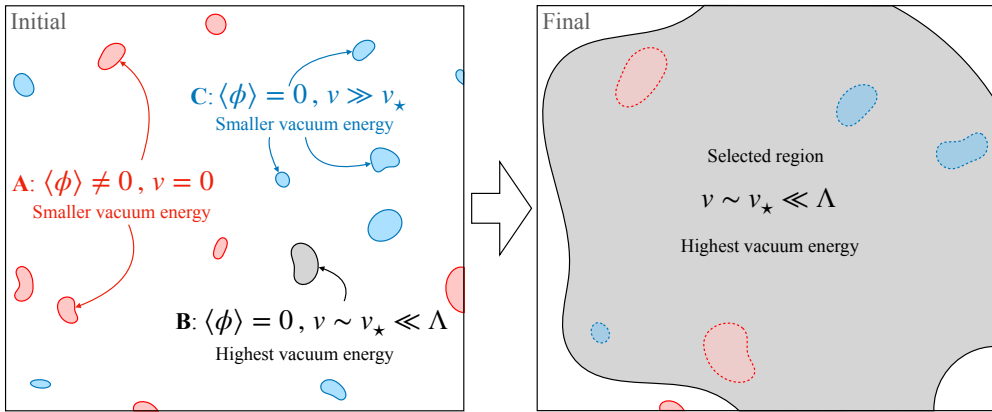


Figure 1: A schematic description of our mechanism. In the left panel, we show causally disconnected patches with different values of the electroweak VEV, v , in an eternally inflating universe. The vacuum energy is maximum in the gray patches labeled B where $v = v_* \ll \Lambda$. These gray regions then expand exponentially faster than other patches. As shown in the right panel, this eventually results in these patches—with a hierarchically small electroweak scale—dominating the volume of the universe. For the red patches where the electroweak VEV vanishes (labeled A) and the blue patches where it is much larger than the observed value v_* (labeled C) the vacuum energy is smaller than that in the gray patches by construction. The red and blue patches with dotted outlines, within the grey region in the right panel, represent such lower energy vacua generated by tunneling from the maximal energy vacuum (see Sec. 2.4). We show the potential for the pseudoscalar and the Higgs doublets in our model corresponding to the three possibilities (A, B, and C) in Fig. 2.

2 A small weak scale from large vacuum energy

2.1 Model

We consider a modified Higgs sector consisting of two Higgs doublets, H_1 and H_2 , and a pseudoscalar, ϕ . We assume that the fundamental theory has a landscape of vacua with varying values of the scalar potential parameters and thus varying values for the electroweak VEV. We then consider an eternally inflating universe where these different vacuum configurations are realized in different causally disconnected patches of the universe.

The pseudoscalar in our model has the following potential,

$$V_\phi(\phi) = \mu_\phi^2 f^2 \left(-\frac{1}{2} \left(\frac{\phi}{f} \right)^2 + \lambda_\phi \left(\frac{\phi}{f} \right)^4 + \dots \right) \quad (2.1)$$

where $\mu_\phi^2 \ll f^2$ and $\lambda_\phi \sim \mathcal{O}(1)$ are both positive. The field value of ϕ in our model never exceeds f so that the above equation presents a consistent effective field theory (EFT) expansion. A potential of the above form can arise if ϕ is the PNGB of a global symmetry

that is spontaneously broken at a scale f , with, $M \sim \sqrt{\mu_\phi f}$, being the scale at which the symmetry is broken explicitly or due to an anomaly.¹

The ‘mexican-hat’ potential, V_ϕ , is minimized at a non-zero value of ϕ and gives a negative contribution to the vacuum energy. The central idea of our mechanism is that the electroweak symmetry breaking can trigger a change in V_ϕ , from a mexican-hat potential to one which is minimised at the origin. This raises the vacuum energy of patches where the electroweak VEV is above some threshold value required to cause such a change in V_ϕ . As in the SM, very large electroweak VEVs, give a large negative vacuum energy contribution to the potential. The net effect of these two factors is that the vacuum energy in our model peaks in patches with a finite but small electroweak VEV. Away from this value, we get a large negative contribution either due to the electroweak or ϕ VEV.

The simplest possibility to realize this would be the addition of a ‘trigger term’ [10] to our potential of the form $V_T \sim |H|^2 \phi^2$. This term can give the desired positive contribution to the pseudoscalar mass. However, such a term is problematic as we can close the Higgs loop to obtain a quadratically divergent term,

$$|H|^2 \phi^2 \rightarrow \frac{\Lambda^2}{16\pi^2} \phi^2. \quad (2.2)$$

This would mean that the change in the $V(\phi)$ that we wish to trigger by the electroweak VEV can already be caused by closing the Higgs loop. The loop-induced effect is in fact bigger than that induced by the Higgs VEV unless, $\Lambda \lesssim 4\pi v$, which kills any hope of solving the hierarchy problem up to high scales.

While cosmological selection models employ diverse mechanisms to select the weak scale, many of them require a term of the form $\phi^n H^\dagger H$ in the potential that is triggered by the electroweak VEV. All such models, therefore, face the issue related to the closing of the Higgs loop, described in the previous paragraph. For our model, we will utilize the minimal solution to this problem provided by Ref. [10], where it was proposed that the operator $H_1^\dagger H_2$ in a two Higgs doublet model (2HDM) can act as the electroweak trigger.² For our model, we thus consider the following trigger term,

$$V_T(\phi, H_1, H_2) = \frac{\mu_\phi^2 f^2}{2} \left(\kappa \left(\frac{H_1^\dagger H_2}{\mu_\phi f} \right) + h.c. \right) \left(\frac{\phi}{f} \right)^2, \quad (2.3)$$

where perturbativity requires,

$$\kappa^2 \lesssim 16\pi^2 \lambda_\phi. \quad (2.4)$$

With this trigger term, it is clearly not possible to generate a one-loop contribution like the one in eq. (2.2). We also impose a \mathbb{Z}_2 symmetry, $H_1 \rightarrow -H_1$ which leads to the following

¹For a PNGB the above potential would arise as a linear combination of periodic terms such as $M^4 \cos \frac{\phi}{f}$, $M^4 \cos \frac{2\phi}{f}$, etc.

²An alternative resolution to this issue can arise if the loop in eq. (2.2) is cutoff at a scale much smaller than the Higgs cutoff, Λ (see for eg. Ref. [3, 21–24]).

2HDM potential,

$$V_{2\text{HDM}}(H_1, H_2) = \mu_1^2 H_1^\dagger H_1 + \mu_2^2 H_2^\dagger H_2 + \lambda_1 (H_1^\dagger H_1)^2 + \lambda_2 (H_2^\dagger H_2)^2 + \lambda_3 (H_1^\dagger H_1)(H_2^\dagger H_2) \\ + \lambda_4 (H_2^\dagger H_1)(H_1^\dagger H_2) + \frac{1}{2} \left(\lambda_5 (H_1^\dagger H_2)^2 + \lambda_5^* (H_2^\dagger H_1)^2 \right). \quad (2.5)$$

Note that apart from κ and λ_5 , all of the coupling above is real by hermiticity. Furthermore, we will assume a real and positive κ , as any accompanying phase can always be removed by rotating H_2 . As far as λ_5 is concerned, we will rewrite it as, $\lambda_5 = \hat{\lambda}_5 e^{i\alpha}$, where $\hat{\lambda}_5 < 0$.

As discussed in Ref. 2.3, the \mathbb{Z}_2 symmetry imposed on $V_{2\text{HDM}}$ is essential to prevent 2HDM potential terms like $(H_1^\dagger H_1)(H_1^\dagger H_2)$, that can, at the two-loop level, generate a contribution like the one in eq. (2.2) by closing the Higgs doublets in eq. (2.3). The \mathbb{Z}_2 symmetry is actually approximate as the trigger term in eq. (2.3) breaks it. In fact, this breaking reintroduces contribution to the ϕ -mass term at the two loop level,³

$$\Delta V_\phi^{2\text{-loop}} \sim \kappa^2 \frac{\mu_\phi^2}{f^2} \frac{\mu_\phi^2}{(16\pi^2)^2} \phi^2. \quad (2.6)$$

Given the upper bound on κ in eq. (2.4), one can check that this contribution is much smaller than that obtained by substituting the electroweak VEV in eq. (2.3)—thus not spoiling the effectiveness of the trigger term.

Collecting all the different terms we thus get the full potential of the Higgs sector,

$$V_H(\phi, H_1, H_2) = V_\phi(\phi) + V_T(\phi, H_1, H_2) + V_{2\text{HDM}}(H_1, H_2). \quad (2.7)$$

2.2 Cosmological set-up and the landscape

We assume that the Higgs sector described in Sec. 2.1 is completely decoupled from the inflaton sector and that the total vacuum energy in a particular minima in the landscape is given by,

$$\mathcal{V}\mathcal{E}^{(ijk)} = \mathcal{V}\mathcal{E}_H(\{\alpha_H^{(i)}\}, P(\phi, H_1, H_2)) + \mathcal{V}\mathcal{E}_\chi(\{\beta_\chi^{(j)}\}, P(\chi)) + (\Lambda_{cc}^{(k)})^4, \quad (2.8)$$

where χ is the inflaton field. The first term denotes the contribution from V_H in eq. (2.7), which vanishes if all the Higgs sector fields are localized at the origin, $\phi = H_1 = H_2 = 0$; the second term denotes the contribution from the inflaton potential which vanishes at $\chi = 0$; and the third term is the contribution of the cosmological constant. Here $\{\alpha_H^{(i)}\}$ denotes a particular choice of Higgs sector parameters, namely $\{\mu_1^2, \mu_2^2, \lambda_1, \lambda_2, \lambda_3, \lambda_4, \lambda_5, \kappa, |\mu_\phi^2|, \lambda_\phi\}$; $\{\beta_\chi^{(j)}\}$ denotes a choice of parameters for the unspecified inflaton potential; and, $\Lambda_{cc}^{(j)}$, is a particular choice for the cosmological constant. The relevant parameters in our theory vary in the range, $-\Lambda^2 < \mu_i^2 < \Lambda^2$ and $-\Lambda^4 < \Lambda_{cc}^4 < \Lambda^4$, across different vacua of the landscape. The scale up to which the hierarchy problem is solved in our model is thus, Λ . Note that

³Note that the term, $\left(\kappa \frac{\mu_\phi}{2f} \frac{\mu_\phi^2}{16\pi^2} H_1^\dagger H_2 + h.c. \right)$ is similarly generated by closing the ϕ -loop in the trigger term. The coefficient of the term is again completely negligible and can be safely ignored for the rest of the analysis.

the mexican hat nature of V_ϕ is crucial to our mechanism and the sign of μ_ϕ^2 in eq. (2.1) is thus assumed to be positive across the landscape. We make no assumptions about the origin of the landscape which can arise either from string theory [25–27] or from a sector at lower energies having multiple scalars (see for eg. Ref [10, 12]).⁴

Our assumption that the Higgs sector and inflaton sector are decoupled from each other is an important one that we now discuss in more detail. In particular we assume (1) that a transition from one vacuum to another in the landscape that alters the Higgs sector parameters, $\{\alpha_H^{(i)}\}$, does not change the inflaton sector parameters, $\{\beta_H^{(j)}\}$ and vice versa; and (2) any coupling between the inflaton, χ and the Higgs sector fields is highly suppressed.

In eq. (2.8), $P(\chi)$ and $P(\phi, H_1, H_2)$, denote the volume-weighted distribution functions for the scalar field values during inflation. We will discuss more about the inflationary dynamics and $P(\chi)$ in Sec. 2.4. For the Higgs sector fields, $P(\phi, H_1, H_2)$ can be computed by solving the volume-weighted Fokker Planck equation (FPV). As we discuss in detail in App. A, a careful analysis of the FPV equation shows that the probability distribution function is sharply peaked at the classical minima of V_H in eq. (2.7) if the following conditions hold,

$$\frac{H_I^4}{v_\star^4} \ll 1, \quad \frac{H_I^4}{\mu_\phi^2 f^2} \ll 1, \quad \frac{f^2}{M_{pl}^2} \ll 1, \quad (2.9)$$

where H_I is the Hubble scale during inflation and $v_\star = 246$ GeV is the observed electroweak VEV. We will assume this to be the case in our model. This assumption simplifies the computation of the vacuum energy contribution from the Higgs sector, $\mathcal{V}\mathcal{E}_H$. In particular, if, for a particular choice of parameters $\{\alpha_H^{(i)}\}$, V_H has a single minimum, we obtain,

$$\mathcal{V}\mathcal{E}_H(\{\alpha_H^{(i)}\}) = V_H(\{\alpha_H^{(i)}\}, \phi_0, H_{1,0}, H_{2,0}) \quad (2.10)$$

where $(\phi_0, H_{1,0}, H_{2,0})$ is the position of the minimum.

We will show in Sec. 2.4 that inflationary dynamics would result in the multiverse being dominated by the vacuum state where each of the terms in eq. (2.8)—and in particular the Higgs contribution, \mathcal{V}_H —is maximized. We expect this maximal vacuum energy to be of the order,

$$H_I^2 M_{pl}^2 \sim \Lambda^4, \quad (2.11)$$

as the maximal value of, Λ_{cc} , is of the order of the cutoff, Λ . The first equation of eq. (2.9) thus implies an upper bound on the cutoff,

$$\Lambda \sim 10^{10} \text{GeV} \sqrt{\frac{H_I}{v_\star}}. \quad (2.12)$$

In the next subsection, we identify the regions in the landscape with maximal $\mathcal{V}\mathcal{E}_H$ and show that they correspond to regions where there is a large hierarchy between the electroweak VEV and the cutoff, Λ .

⁴Note that, for our selection mechanism to work, we require an exponentially large number of vacua to ensure that the electroweak VEV is scanned finely in the landscape. This is not, however, a severe issue because the number of vacua in the landscape also grows exponentially with the number of scalars.

2.3 Maximisation of vacuum energy

We now show that if the parameters of the potential are varied the vacuum energy contribution, $\mathcal{V}\mathcal{E}_{\mathcal{H}}$, from the Higgs sector is maximized for a small but finite electroweak VEV. We show this in two steps. First, we consider the variation of μ_1^2 and μ_2^2 , keeping all the quartics fixed. This will give us some restrictions that must be imposed on the quartics for our mechanism to be successful. In the next step, we will also vary the quartics and show how the regions allowed by the above conditions are automatically selected by our mechanism. As far as the parameters in eq. (2.1) are concerned, as already mentioned we must require the sign of μ_ϕ^2 to be fixed across the landscape. As far as the magnitude of, μ_ϕ^2 and f , are concerned we keep them also fixed in the following analysis for the sake of simplicity. As we will see later, however, the impact of varying these two quantities can be understood in a straightforward way.

Step 1: Variation of μ_1^2 and μ_2^2

To evaluate, $\mathcal{V}\mathcal{E}_{\mathcal{H}}$, in different regions of the landscape, we classify the possible local minima of V_H into three classes: (i) minima with electroweak symmetry preserved (which necessarily requires $\langle\phi\rangle \neq 0$), (ii) minima with electroweak symmetry broken and $\langle\phi\rangle \neq 0$ and (iii) minima with electroweak symmetry broken and $\langle\phi\rangle = 0$. We then evaluate the vacuum energy contribution for each case. We will see that the vacuum energy will peak for the last class of minima in regions of the landscape with a hierarchically small electroweak scale. Before carrying out such an analysis we must assume that the potential is bounded from below. This requires,

$$\lambda_3 + \lambda_4 + \hat{\lambda}_5 + 2\sqrt{\lambda_1\lambda_2} \geq 0, \quad (2.13)$$

for $\lambda_4 + \hat{\lambda}_5 < 0$ and $\lambda_3 \geq -2\sqrt{\lambda_1\lambda_2}$ for $\lambda_4 + \hat{\lambda}_5 > 0$.

Class I – Electroweak symmetry preserved : We first consider the case where $\langle H_1 \rangle = \langle H_2 \rangle = 0$ so that the trigger term is not effective. In these regions, ϕ has a mexican hat potential that is minimized at,

$$\langle\phi\rangle = \pm \frac{f}{\sqrt{4\lambda_\phi}}. \quad (2.14)$$

$\mathcal{V}\mathcal{E}_{\mathcal{H}}$ in this region only comes from V_ϕ and is given by,

$$\mathcal{V}\mathcal{E}_{\mathcal{H}}^I = -\frac{\mu_\phi^2 f^2}{16\lambda_\phi}. \quad (2.15)$$

Note that these solutions correspond to minima only if both μ_1^2 and μ_2^2 are positive.

Class II – EW symmetry broken and $\langle\phi\rangle \neq 0$: To analyze this possibility we use the minimization condition with respect to the scalar ϕ , i.e. $\partial V_H/\partial\phi = 0$, to obtain,

$$\hat{\phi}^2 = \frac{f^2}{4\lambda_\phi} - \frac{\kappa f}{4\lambda_\phi\mu_\phi} (H_1^\dagger H_2 + h.c.) \quad (2.16)$$

and then substitute this in the full potential,

$$V_H(\phi, H_1, H_2)|_{\phi \rightarrow \hat{\phi}} = -\frac{\mu_\phi^2 f^2}{16\lambda_\phi} + \hat{V}_{2HDM}(H_1, H_2). \quad (2.17)$$

Here $\hat{V}_{2HDM}(H_1, H_2)$ is a 2HDM potential with the quartics in eq. (2.5) modified,

$$\lambda_4 \rightarrow \lambda_4 - \frac{\kappa^2}{8\lambda_\phi} \quad \lambda_5 \rightarrow \lambda_5 - \frac{\kappa^2}{8\lambda_\phi} \quad (2.18)$$

and an additional term,

$$\frac{\kappa\mu_\phi f}{8\lambda_\phi} H_1^\dagger H_2 + h.c. \quad (2.19)$$

We show in App. B that if a minimum exists for \hat{V}_{2HDM} , its contribution to the vacuum energy would be negative making the total vacuum energy in these local minima to be smaller than the value for class I minima given by eq. (2.15). On the other hand, \hat{V}_{2HDM} has a runaway direction, and no EW breaking minima, if,

$$\lambda_3 + \lambda_4 - \frac{\kappa^2}{8\lambda_\phi} - \left| \lambda_5 - \frac{\kappa^2}{8\lambda_\phi} \right| \leq -2\sqrt{\lambda_1\lambda_2}. \quad (2.20)$$

and $\lambda_4 + \hat{\lambda}_5 < 0$. Class II minima are thus disallowed if the condition in eq. (2.20) is satisfied. Note that the left-hand side above is a monotonically decreasing function of κ so that for a large enough κ , eq. (2.20) this is guaranteed to be true.

Class III – Electroweak symmetry broken and $\langle \phi \rangle = 0$: In regions of the landscape where $\langle H_1^\dagger H_2 \rangle \neq 0$, the trigger term gives a new contribution to the ϕ^2 term. This can change the shape of the ϕ -potential from a mexican hat to one with a minimum at $\phi = 0$, if,

$$-\mu_\phi^2 + \frac{\kappa\mu_\phi}{f} \langle (H_1^\dagger H_2 + h.c.) \rangle \geq 0. \quad (2.21)$$

The scalar then gets stabilized at $\phi = 0$ and the trigger term becomes ineffective giving no additional contribution to the 2HDM potential given by eq. (2.5). As we will soon show, this is the class of minima that will be selected by our mechanism.

With $\langle \phi \rangle = 0$, we must minimise V_{2HDM} . As we discuss in App. B, the VEVs of the doublets must take one of the following forms [28],

$$\langle H_1 \rangle = \frac{1}{\sqrt{2}} \begin{pmatrix} 0 \\ v_1 \end{pmatrix}, \quad \langle H_2 \rangle = \frac{1}{\sqrt{2}} \begin{pmatrix} 0 \\ v_2 e^{i\xi} \end{pmatrix}; \quad (2.22)$$

$$\langle H_1 \rangle = \frac{1}{\sqrt{2}} \begin{pmatrix} 0 \\ v_1 \end{pmatrix}, \quad \langle H_2 \rangle = \frac{1}{\sqrt{2}} \begin{pmatrix} u \\ 0 \end{pmatrix} \quad (2.23)$$

where $u, v_1, v_2 > 0$. The first possibility is realized if and only if,

$$\lambda_4 + \hat{\lambda}_5 < 0, \quad (2.24)$$

whereas the second possibility is realized if $\lambda_4 + \hat{\lambda}_5 > 0$.⁵ Note, however, that in our set-up the second possibility is not consistent with eq. (2.21) as it gives $\langle H_1^\dagger H_2 \rangle = 0$. This implies that for, $\lambda_4 + \hat{\lambda}_5 > 0$, there are no stable class III minima.

Assuming eq. (2.24) holds so that the doublet VEVs are given by eq. (2.22), we can now minimize with respect to ξ to obtain, $\langle 2\xi + \alpha \rangle = 0$ where α is the phase of λ_5 defined below eq. (2.5) (see App. B). Next, we can minimize the potential in the two CP-even, charge-neutral directions to obtain v_1 and v_2 as a function of μ_1^2, μ_2^2 and the quartics; these minimization conditions have been provided in eq. (B.12) of App. B. Using these conditions we can trade μ_1^2 and μ_2^2 for v_1 and v_2 —or equivalently for $v = \sqrt{v_1^2 + v_2^2}$ and $\tan \beta = v_2/v_1$ (see eq. (B.13)).

As V_ϕ does not contribute to the vacuum energy, the vacuum energy contribution, $\mathcal{V}\mathcal{E}_{\mathcal{H}}$, for class III comes only from eq. (2.5) and is given by (see App. B),

$$\mathcal{V}\mathcal{E}_{\mathcal{H}}^{III} = -\frac{1}{4}(\lambda_1 c_\beta^4 + \lambda_2 s_\beta^4 + \lambda_{345} s_\beta^2 c_\beta^2) v^4, \quad (2.25)$$

where $\lambda_{345} = \lambda_3 + \lambda_4 + \hat{\lambda}_5$, $s_\beta = \sin \beta$ and $c_\beta = \cos \beta$. The minimization conditions in eq. (B.13) imply that as μ_1^2 and μ_2^2 vary in the landscape, v and $\tan \beta$ also vary. Let us now find the maximum value of $\mathcal{V}\mathcal{E}_{\mathcal{H}}^{III}$ as v and $\tan \beta$ are varied. It is clear that for a given value of β the vacuum energy in eq. (2.25) monotonically decreases with increasing v . The maximal value of the vacuum energy is thus attained for the smallest value of v allowed by eq. (2.21),

$$v^2 \geq \frac{\mu_\phi f}{\kappa s_\beta c_\beta}. \quad (2.26)$$

For a given value of $\tan \beta$ this gives the following upper bound for the vacuum energy for class III minima,

$$\mathcal{V}\mathcal{E}_{\mathcal{H}}^{III} \leq -\frac{1}{4}(\lambda_1 c_\beta^4 + \lambda_2 s_\beta^4 + \lambda_{345} s_\beta^2 c_\beta^2) \frac{\mu_\phi^2 f^2}{\kappa^2 s_\beta^2 c_\beta^2}. \quad (2.27)$$

Next, we maximize with respect to $\tan \beta$ to obtain the maximal value for the vacuum energy for class III minima,

$$\mathcal{V}\mathcal{E}_{\mathcal{H}}^{III,max} = -\frac{\mu_\phi^2 f^2}{4\kappa^2} (\lambda_{345} + 2\sqrt{\lambda_1 \lambda_2}) \quad (2.28)$$

which is realized in the following region of the landscape,

$$v_\star^2 = \frac{\mu_\phi f}{\kappa s_{\beta_\star} c_{\beta_\star}}, \quad \tan^2 \beta_\star = \sqrt{\frac{\lambda_1}{\lambda_2}} \quad (2.29)$$

which can also be written in terms of $\mu_{1\star}^2$ and $\mu_{2\star}^2$ —the value of the underlying parameters at this point—by inverting eq. (B.13).

Notice that the value for the electroweak VEV in eq. (2.29) can be much smaller than the cutoff $\Lambda \sim \sqrt{H_I M_{pl}}$ (see eq. (2.11)),

$$v_\star^2 \ll \Lambda^2, \quad (2.30)$$

⁵For $\lambda_4 + \hat{\lambda}_5 = 0$ we get a flat direction in the EM breaking direction.

as $M \sim \sqrt{\mu_\phi f}$ —the global symmetry breaking scale associated with the PngB ϕ —can be naturally small. In fact, if we allow the magnitude of μ_ϕ^2 and f to vary in the landscape while keeping the sign of the former fixed, the vacua with the smallest value of $\mu_\phi f$ will be selected as they will correspond to the highest value of $\mathcal{V}\mathcal{E}_H^{III,max}$.

We will now show that the region of the landscape defined by eq. (2.29) can have the highest vacuum energy contribution, $\mathcal{V}\mathcal{E}_H$, not only among class III minima but in the whole landscape, provided certain conditions are satisfied by the quartics. The desired region given by eq. (2.29) will then be selected by our mechanism. The first of these conditions arises from requiring that $\mathcal{V}\mathcal{E}_H^{III,max}$ exceeds the vacuum energy for class I minima, $\mathcal{V}\mathcal{E}_H^I$ which gives,

$$\kappa^2 > 4\lambda_\phi(\lambda_{345} + 2\sqrt{\lambda_1\lambda_2}). \quad (2.31)$$

We will demand one more condition on the quartics to ensure that eq. (2.29) is the region with maximal vacuum energy in the whole landscape. We want to eliminate the possibility of the coexistence of multiple local minima for a given choice of the parameters, $\{\alpha_H^i\}$. This is important because, for more than one minimum, the vacuum energy computation would involve solving the FPV equation to obtain the relative probability of the fields to be in the different minima; in particular eq. (2.28) is not valid if there are other coexisting minima. We show in App. B that for a given choice of parameters, $\{\alpha_H^i\}$, class III minima cannot coexist with class I minima. On the other hand, class II and III minima may coexist. If the condition in eq. (2.20) is imposed, however, stable class II minima are disallowed. In this case, only class I and III minima can exist—and if eq. (2.31) is satisfied—the class III minima satisfying eq. (2.29) will have the maximal vacuum energy in the whole of the landscape.

To sum up, we have shown that the region of the landscape defined by eq. (2.29) has the maximal vacuum energy in the whole landscape if the following conditions are met:

- the potential is bounded from below which requires eq. (2.13), i.e., eq. (2.13) is satisfied
- class III minima exist, which requires eq. (2.24),
- the maximal vacuum energy of the class III minima exceeds that of class I minima, $\mathcal{V}\mathcal{E}_H^{III,max} > \mathcal{V}\mathcal{E}_H^I$ which gives eq. (2.31), and,
- class II minima do not exist which is implied by eq. (2.20).

We illustrate the basic idea of our mechanism in Fig. 2 where we show the shape of the scalar potentials as the electroweak VEV is varied. We show only class I and III minima in Fig. 2 assuming eq. (2.20) is obeyed. Given eq. (2.20), a positive μ_1^2 and μ_2^2 results in class I minima whereas even if one of these two parameters is negative only class III minima can be obtained. In the panel on the left, we show the situation when the electroweak VEV is zero and the pseudoscalar has a mexican hat potential. In the middle panel, the electroweak VEV is at the threshold value given by eq. (2.29) such that the ϕ -potential is minimized at the origin. If the vacuum energy in the middle panel has to be larger than the one in the

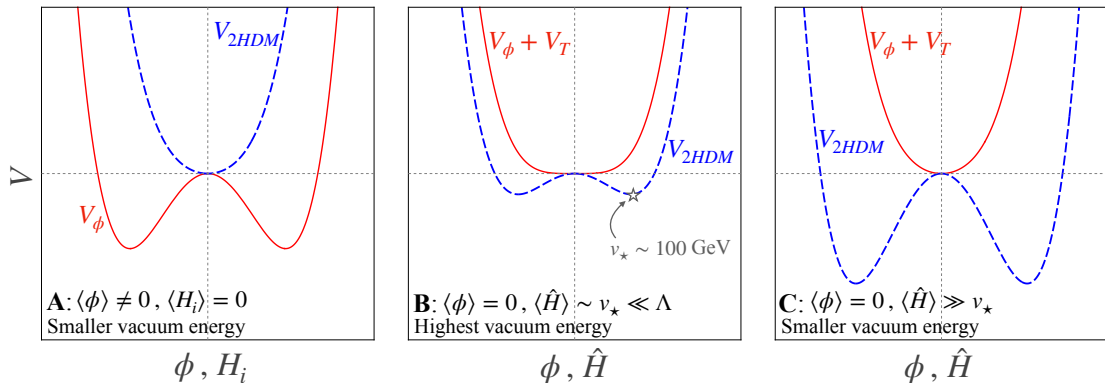


Figure 2: The potential of ϕ and the Higgs doublets for varying values of the electroweak VEV, v . In the left panel, we show a class I minimum with $v = 0$ and a mexican hat potential for ϕ . H_i in this case can be any of the 8 components of the 2 Higgs doublets. In the middle panel, we take, $v = v_*$, the threshold value required to change the ϕ -potential to one with its minimum at the origin. In the right panel we show that for, $v \gg v_*$, while the ϕ -potential is still minimized at the origin, the Higgs potential becomes deeper. In the middle and right panel, the minima are of the class III category and $\hat{H} = \sqrt{\phi_3^2 + \phi_7^2}$, where ϕ_3 and ϕ_7 are the two CP even components (see eq. (B.1)). The middle panel clearly corresponds to vacua with maximal vacuum energy. The three scenarios have been labeled A, B, and C as they directly correspond to the three similarly labeled categories of vacua in Fig. 1.

left panel, the gain in vacuum energy due to the rising of the ϕ minima must be larger than the negative contribution from the electroweak VEV; it is precisely this requirement that yields eq. (2.31). Finally, on the right, we show that as the electroweak VEV increases the Higgs minimum becomes deeper resulting in a monotonically decreasing vacuum energy contribution as in the SM. Thus the maximal value of the vacuum energy contribution, $\mathcal{V}\mathcal{E}_{\mathcal{H}}$, is attained in the middle panel where the electroweak VEV is much smaller than the cutoff and the ϕ resides at the origin. This region then expands exponentially faster than other regions of the landscape to eventually occupy almost all of the multiverse—thus resolving the hierarchy problem.

Step 2: Variation of the quartics

We will now show that if the quartics, λ_{1-5} and κ are varied, we do not need to impose the conditions on the quartics listed in step 1, as the regions of the landscape satisfying them would be automatically selected by our mechanism. First, regions of the multiverse where eq. (2.13) is not obeyed have a runaway direction in field space which would result in a big crunch. Next, in regions of the landscape where, eq. (2.24) or eq. (2.31), is not satisfied either class III minima do not exist at all or they have vacuum energy less than that of class I minima.

In regions where the last condition, i.e. eq. (2.20) is not satisfied, class II minima become possible. As we have already mentioned, and discussed in detail in App. B, such

minima will always have vacuum energy smaller than $\mathcal{V}\mathcal{E}_{\mathcal{H}}^I$ and, if eq. (2.31) is satisfied, also smaller than $\mathcal{V}\mathcal{E}_{\mathcal{H}}^{III,max}$. It is possible, however, for a class II minimum to coexist with a class III minimum having higher vacuum energy. We would then need to obtain $P(\phi, H_1, H_2)$ from the FPV equation to compute the vacuum energy. An upper bound on the vacuum energy in this scenario can be obtained by considering a $P(\phi, H_1, H_2)$ that peaks entirely on the higher class III minimum; we can then use the expression for $\mathcal{V}\mathcal{E}_{\mathcal{H}}^{III,max}$ in eq. (2.28) to compute this upper bound. The value of $\mathcal{V}\mathcal{E}_{\mathcal{H}}^{III,max}$, however, would be higher in regions where eq. (2.20) is respected compared to regions where this condition is violated. The reason for this is that the left hand side of eq. (2.20) is a monotonically decreasing function of κ so that regions obeying this condition will have a higher κ and thus a higher, $\mathcal{V}\mathcal{E}_{\mathcal{H}}^{III,max}$ (see eq. (2.28)).

Thus the regions of the landscape satisfying the conditions, eq. (2.13), eq. (2.24), eq. (2.31), and eq. (2.20), have larger vacuum energy than regions violating them. Our mechanism, therefore, automatically selects them.

2.4 Volume of desired region

We have established that in our model the maximum vacuum energy is attained in parts of the landscape where the electroweak VEV is finite but much smaller than the cutoff. We now wish to quantitatively show that, after a sufficiently long time, these regions with maximal vacuum energy given by, $\mathcal{V}\mathcal{E}_{\mathcal{H}}^{III,max}$ in eq. (2.28), dominate the multiverse in volume over other regions.

Following Ref. [29], we first show that the universe is dominated by the maximal energy vacuum state in the landscape, that we call $\lambda_* = \{i_*, j_*, k_*, m_*\}$, where i_* and j_* respectively specify the choice of parameters in the Higgs sector and the inflaton sector; k_* denotes the choice of the cosmological constant; and m_* labels the highest vacuum of the inflaton, χ (see eq. (2.8)). The volume weighted probability distribution functions for the different vacua in the landscape obey the following differential equations (see for eg. Ref. [29] and the references therein),

$$\frac{dP_*}{dt} = - \sum_{\lambda}^{\lambda \neq \lambda_*} \Gamma_{\lambda_* \rightarrow \lambda} P_* + \sum_{\lambda}^{\lambda \neq \lambda_*} \lambda \Gamma_{\lambda \rightarrow \lambda_*} P_{\lambda} + 3H_* P_* \quad (2.32)$$

$$\frac{dP_{\lambda}}{dt} = - \sum_{\mu}^{\mu \neq \lambda} \Gamma_{\lambda \rightarrow \mu} P_{\lambda} + \sum_{\mu}^{\mu \neq \lambda, \lambda_*} \Gamma_{\mu \rightarrow \lambda} P_{\mu} + \Gamma_{\lambda_* \rightarrow \lambda} P_* + 3H_{\lambda} P_{\lambda} \quad (2.33)$$

where P_{λ} is the volume-weighted probability to be in the state λ , $P_* = P_{\lambda_*}$ is the volume-weighted probability to be in the maximal energy vacuum and H_* is the corresponding Hubble scale. The transition rates from one vacuum to another, $\Gamma_{\alpha \rightarrow \beta}$, are, as we will soon discuss, (doubly) exponentially suppressed numbers. Thus we can take H_* to be larger than all other parameters appearing in the above equations. This results in P_* dominating over the other P_{λ} so that, the last term in the right hand side (RHS) of eq. (2.32) and the third term in the RHS of eq. (2.33), become the dominant terms. The solution to these

equations is found to have the following form for large times,

$$P_\star(t) = P_\star(0)e^{3H_\star t}, \quad P_\lambda(t) = \frac{\Gamma_{\lambda_\star \rightarrow \lambda}}{H_\star} P_\star(t). \quad (2.34)$$

As $\Gamma_{\lambda_\star \rightarrow \lambda}/H_\star \ll 1$, we see that the maximal energy vacuum, λ_\star , dominates over all others. The inflationary Hubble scale, H_I , in Sec. 2.2 should thus be identified with the Hubble scale in this vacuum, i.e. $H_I = H_\star$. The maximal energy vacuum, λ_\star , is the one for which all the terms in eq. (2.8), including in particular the Higgs-sector contribution, $\mathcal{V}\mathcal{E}_H$, are independently maximized.⁶ In this vacuum, the electroweak VEV is thus given by eq. (2.29) and is much smaller than the cutoff. We see that all the, P_λ , eventually enter a stationary regime where they grow at the same rate, $e^{3H_\star t}$. This is because regions in a vacuum state, $\lambda \neq \lambda_\star$, primarily arise due to tunneling from the maximal energy vacuum.

In order to give rise to a universe such as ours the inflaton sector must transition to vacua, $\lambda_\star \rightarrow \lambda_{slow}$, which permit a slow-roll and reheating phase. The total volume of such universes are given by,

$$\mathcal{V}(t) = \sum_{\lambda_{slow}} P_\star(0)e^{3H_\star(t-t_+)} \Gamma_{\lambda_\star \rightarrow \lambda_{slow}} e^{N_{slow}} r_V(t_{age}) \Theta(t - t_+) \quad (2.35)$$

where t_{age} is the age of the universe since reheating and $r_V(t_{age})$ is the factor by which the universe has expanded in this time period; N_{slow} and t_{slow} are, respectively, the number of e-folds and the time elapsed during the slow-roll phase in the vacuum λ_{slow} ; $\Gamma_{\lambda_\star \rightarrow \lambda_{slow}}$ is the rate for the transition, $\lambda_\star \rightarrow \lambda_{slow}$, and $t_+ = t_{age} + t_{slow}$. The theta function arises because a minimum time, t_+ , is required before any universe of an age, t_{age} , can emerge. Our assumption of complete decoupling between the Higgs and inflaton sector (see Sec. 2.2) becomes crucial here and implies that the transition, $\lambda_\star \rightarrow \lambda_{slow}$ —or more explicitly $\{i_\star, j_\star, k_\star, m_\star\} \rightarrow \{i_\star, j_{slow}, k_{slow}, m_{slow}\}$ —does not result in a change in the Higgs sector parameters, $\{\alpha_H^i\}$, and the electroweak VEV remains, $v_\star^2 \ll \Lambda^2$, given by eq. (2.29). Note that number of e-folds in slow-roll phase need not be exponentially large in our model.

We now compute the volume of the regions of the multiverse that undergo slow-roll and reheating but with $v \neq v_\star$. Using again our assumption of decoupling between the Higgs and inflaton sectors, we see that these regions will emerge from the maximal energy vacuum λ_\star after two transitions, i.e. $\lambda_\star \rightarrow \lambda' \rightarrow \lambda'_{slow}$ —or written explicitly $\{i_\star, j_\star, k_\star, m_\star\} \rightarrow \{i', j_\star, k', m_\star\} \rightarrow \{i', j_{slow}, k'_{slow}, m_{slow}\}$ —where the first one changes Higgs sector parameters and the cosmological constant but not the inflaton sector parameters. The second transition, on the other hand, changes the inflaton sector parameters and the cosmological constant but not the Higgs sector parameters. Note that the inflaton sector in the vacuum states, λ_\star and λ' , are identical up to a difference in the cosmological constant, $\Delta\Lambda_{cc}$. This is also the case for the vacua, λ_{sol} (in eq. (2.35)), and λ'_{sol} and the difference in cosmological constants is, in fact, identical to the previous case, i.e. $\Delta\Lambda_{cc}$.

⁶Here we are assuming that for the maximal value of the cosmological constant, $\Lambda_{cc}^{(k_\star)}$ the full range of variation in the parameters, $\{\alpha_H^{(i)}\}$, and, $\{\beta_\chi^{(j)}\}$ in eq. (2.8), is realized in the landscape.

This implies that the transition rates, $\Gamma_{\lambda_\star \rightarrow \lambda_{slow}}$ and $\Gamma_{\lambda' \rightarrow \lambda'_{slow}}$, are equal. For the volume arising after the first transition, we get,

$$P'(t) = \sum_{\lambda'} P_\lambda(t) = \sum_{\lambda'} \frac{\Gamma_{\lambda_\star \rightarrow \lambda'}}{H_\star} P_\star(t). \quad (2.36)$$

Note that this volume is exponentially smaller than, $P_\star(t)$, despite the fact that the summation above may run over an exponentially large number of states (for a system of n scalars the number of vacua scales as e^n). This is because the tunneling rate $\Gamma_{\lambda_\star \rightarrow \lambda'}$ is suppressed by the double exponential, e^{-S} , where the action S is itself an exponentially large ratio of energy scales raised to the fourth power.⁷ Even in the string theory landscape, while the number of vacua has been estimated to be as large as 10^{500} [30], the estimate for the probabilities, $e^{-10^{122}}$ [25], is exponentially smaller.

We can again compute the volume of the universes arising from $P'(t)$ that undergo a slow-roll and reheating phase by considering the second transition, $\lambda' \rightarrow \lambda'_{slow}$,

$$\mathcal{V}'(t) = \sum_{\lambda'_{slow}} P'(t - t_+) \Gamma_{\lambda_\star \rightarrow \lambda_{slow}} e^{N'_{slow} r_V(t_{age})} \Theta(t - t'_+), \quad (2.37)$$

where we have used, $\Gamma_{\lambda' \rightarrow \lambda'_{slow}} = \Gamma_{\lambda_\star \rightarrow \lambda_{slow}}$. Here, N'_{slow} and t'_{slow} , the number of e-folds and slow-roll time in the vacuum state, λ'_{slow} , are smaller than the corresponding quantities, N_{slow} and t_{slow} , in eq. (2.35). To show this, we first note that the vacuum energy of, λ'_{slow} , is smaller than the vacuum energy of λ_{slow} . This follows from the fact that although the change in vacuum energy for the $\lambda_\star \rightarrow \lambda_{slow}$ transition is the same as that in the $\lambda' \rightarrow \lambda'_{slow}$ transition, the vacuum λ_\star has greater vacuum energy than λ' by definition. Thus, despite the inflaton potential being the same in both cases, the Hubble parameter in λ'_{slow} is smaller than that in λ_{slow} resulting in a shorter slow roll time and smaller number of e-folds.

We must address a final subtlety before quantifying the volume in the multiverse with a large electroweak hierarchy. We want to compare this volume with the volume without such a hierarchy for some large time, t . There is, however, no well-defined way of choosing time slices across the causally disconnected patches in the multiverse which leads to the so-called measure problem. In the calculation of $\mathcal{V}(t)$ and $\mathcal{V}'(t)$ we have been implicitly using the proper time cutoff measure where the time slices are chosen according to the proper time elapsed in each patch. This measure however leads to the so-called youngness paradox [20]. This can be understood directly from, eq. (2.35), if we compare volumes for universes with different values of t_{age} . We see that a smaller value of t_{age} yields a smaller t_+ and thus an exponentially larger volume. Thus younger universes are exponentially favoured in the proper time cutoff measure which results in this paradox. The paradox can be restated as an exponential preference for a higher than observed CMB temperature [31] which observationally rules out the proper time cutoff measure.

Here we will use the stationary measure [29] which evades the youngness paradox as well as other issues such as a gauge dependence on the time parameterization and the Boltzmann brain problem [32, 33]. In the stationary measure we shift the time coordinate

⁷We thank S. Trivedi for explaining this point to us.

such that volumes are evaluated only as a function of the time elapsed since the beginning of the stationary regime. In our case, we obtain for the two volumes in eq. (2.35) and eq. (2.37) in the stationary measure,

$$\begin{aligned}\mathcal{V}(t)_{stationary} &= \mathcal{V}(t)|_{t \rightarrow t+t_+} \\ \mathcal{V}'(t)_{stationary} &= \mathcal{V}'(t)|_{t \rightarrow t+t'_+}\end{aligned}\tag{2.38}$$

This removes the dependence of $\mathcal{V}(t)_{stationary}$ on t_+ and thus there is no youngness paradox in the stationary measure. We can now evaluate the ratio of the latter volume to the former for large values of t ,

$$\lim_{t \rightarrow \infty} \frac{\mathcal{V}'(t)_{stationary}}{\mathcal{V}(t)_{stationary}} \ll 1\tag{2.39}$$

where we have used $N'_{slow} < N_{slow}$ and the arguments below eq. (2.36).⁸ This shows that in the stationary measure, after a sufficiently long time, the volume of the multiverse is dominated by regions where the electroweak scale is given by eq. (2.29) and is thus hierarchically smaller than the cutoff, Λ .

3 Phenomenology of the 2HDM sector

The phenomenology of the 2HDM sector provides an opportunity to test the most important prediction of our model, namely that of the value of $\tan \beta$,

$$\tan^4 \beta = \left(\frac{\lambda_1}{\lambda_2} \right),\tag{3.1}$$

derived in eq. (2.29). Indeed, using the standard expressions for the masses and mixing angles of the different Higgs bosons (see for eg. Ref. [34]) one can convert the above equation into the following prediction,

$$\cos \alpha = \sqrt{\frac{m_h^2 - m_H^2 \tan^2 \beta}{(m_h^2 - m_H^2)(1 + \tan^2 \beta)}}.\tag{3.2}$$

that connects, α , the mixing angle between the CP-even Higgs bosons to $\tan \beta$ and m_H , the mass of the heavier CP even Higgs. These are all observables that can be independently measured. While m_H can be measured by directly producing H at LHC, the measurement of the couplings of the charged Higgs, H^\pm , and pseudoscalar, A , can determine $\tan \beta$. For a given value of $\tan \beta$, a measurement of the couplings of the SM-like Higgs, h , can then determine α .

We show this graphically in Fig. 3 where contours of $\cos(\beta - \alpha)$ predicted by eq. (3.1) have been shown on the $\tan \beta$ - m_H plane. Note that, $\cos(\beta - \alpha)$, is crucial in determining

⁸Note that we have not addressed the cosmological constant problem in our discussion so far. We would like to emphasize that our mechanism is completely compatible with Weinberg's anthropic solution to the cosmological constant problem [18]. We can ensure that the final cosmological constant is in the anthropic range by multiplying both $\mathcal{V}(t)_{stationary}$ and $\mathcal{V}'(t)_{stationary}$ by anthropic suppression factors. Assuming these factors are of the same order, our conclusion in eq. (2.39) would remain unchanged.

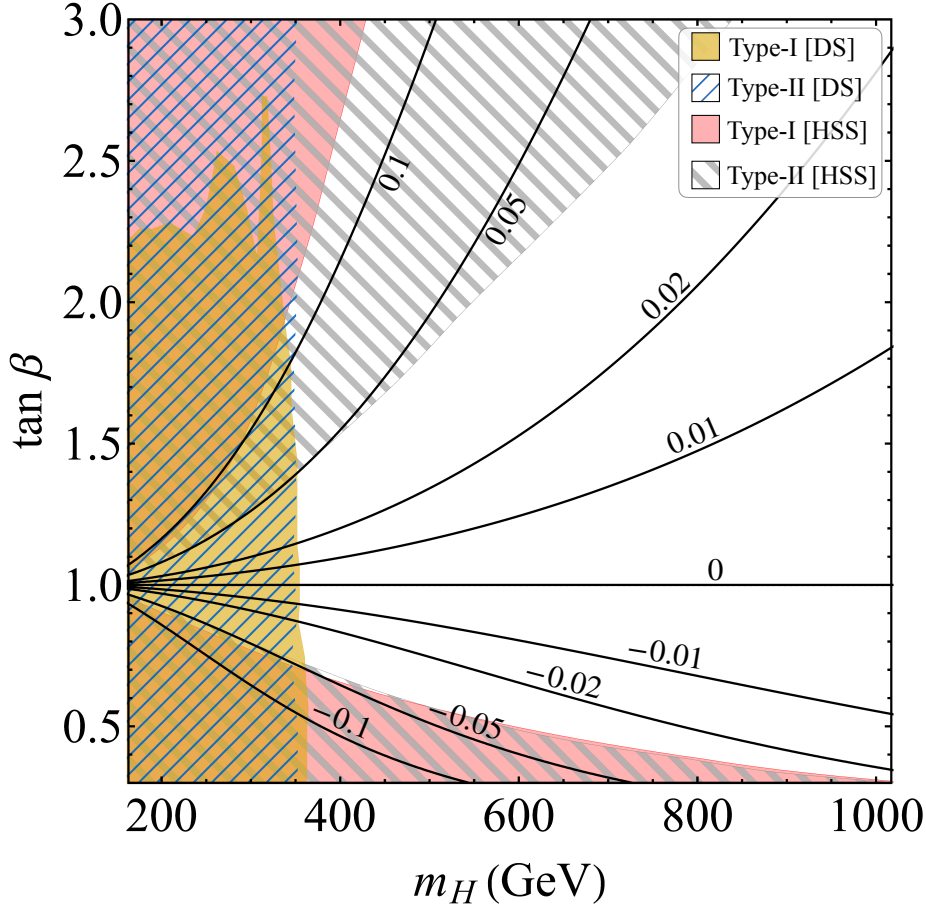


Figure 3: The 2HDM parameter space for our model in the $\tan\beta$ - m_H plane. The black contours show predictions for $\cos(\beta - \alpha)$ as a function of m_H and $\tan\beta$. These predictions can be verified by measurement of the couplings of the SM-like Higgs whose deviations from SM are controlled by $\cos(\beta - \alpha)$. We show the values of $\cos(\beta - \alpha)$ excluded by Higgs signal strength (HSS) measurements for both Type I (pink) and Type II models (gray hatched). We also show direct search (DS) bounds for Type-1 (blue hatched) and Type-2 (brown) models (see text for details).

the deviations of the couplings of the lighter Higgs, h , from SM values. In particular $\cos(\beta - \alpha) = 0$ is the alignment limit where couplings of the h exactly match SM values. Too-large values of $\cos(\beta - \alpha)$ are thus excluded by Higgs signal strength measurements; Fig. 3 shows the resulting bounds obtained by Ref. [35, 36]. Bounds for Type I models where only H_1 couples to all the fermions have been shown separately from bounds on Type II models where H_2 couples to up-type fermions and H_1 couples to down type fermions and leptons. We have shown only $\mathcal{O}(1)$ values of $\tan\beta$ motivated by eq. (3.1) as much larger or smaller values will require a large hierarchy in the values of λ_1 and λ_2 .

In Fig. 3 we also show the direct search bounds on the 2HDM parameter space. The hatched region shows the direct search bounds on H and A presented in Ref. [34], These

arise from the processes $H \rightarrow \gamma\gamma$ and $H/A \rightarrow \tau\tau$. For the latter process, the pseudoscalar and heavy CP even Higgs masses have been assumed to be equal, i.e. $m_A = m_H$. This assumption results in conservative bounds as m_A can be independently varied in our model and a larger m_A which would result in weaker bounds. As far as the charged Higgs is concerned, the most stringent bounds arise from $b \rightarrow s$ processes [34]. For a given $\tan\beta$, these can be always satisfied by choosing a large enough charged Higgs mass m_{H^\pm} . While this requires somewhat large absolute values of the coupling $|\lambda_{45}| = |\lambda_4 + \lambda_5|$ in certain regions of the parameter space—for instance, we require $|\lambda_{45}| > 15$ for $\tan\beta < 0.8$ ($\tan\beta < 1$) in Type II (Type I) models—this is still well within the perturbativity bound on the quartics, $\lambda_i \lesssim 16\pi^2$.

4 Phenomenology of ϕ and dark matter

The pseudoscalar, ϕ , in our model, is a light weakly coupled state with its mass and couplings suppressed by powers of f . As the $\phi \rightarrow -\phi$ symmetry remains unbroken in our selected vacua, the ϕ couples quadratically to SM fields. These quadratic couplings,

$$\mathcal{L}_{\phi^2 SM} = -c_e \frac{\phi^2}{f^2} m_e \bar{e}e - c_q \frac{\phi^2}{f^2} m_q \bar{q}q + c_\gamma \frac{\phi^2}{f^2} \frac{\alpha_{em}}{4\pi} F_{\mu\nu} F^{\mu\nu} + c_g \frac{\phi^2}{f^2} \frac{\alpha_s}{4\pi} G_{\mu\nu}^a G^{a,\mu\nu} \quad (4.1)$$

can, for instance, be generated via a tree-level Higgs exchange due to the trigger term in eq. (2.3). The observational and experimental bounds on such quadratically coupled light fields are negligible unless there is a background classical configuration of ϕ (see for instance Ref. [37]). We will thus study how a classical background configuration of ϕ can arise due to the misalignment mechanism. We will also show that in certain regions of the parameter space, ϕ can account for the observed dark matter relic density.

As far as the mass of ϕ is concerned, an additional subtlety is introduced by the fact that, in our model, it is actually smaller than the naive expectation, $\mathcal{O}(\mu_\phi^2)$. This is because the mass of ϕ is given by,

$$m_\phi^2 = \left(-\mu_\phi^2 + \kappa \frac{\mu_\phi}{f} v_\star^2 s_{\beta_\star} c_{\beta_\star} \right), \quad (4.2)$$

where a cancellation takes place between the two terms above in the selected vacua (see eq. (2.29)). The cancellation between the two terms on the right-hand side, however, is only approximate as κ , and the 2HDM parameters are scanned in the landscape in discrete steps so that the second term above also takes a discrete set of values. To take into account this fact we take $m_\phi^2 = \epsilon^2 \mu_\phi^2$, where, $\epsilon \ll 1$, is a parameter that captures the degree of cancellation between the two terms—which in turn depends on how finely the underlying Higgs sector parameters are being scanned. In particular, the limit of continuous scanning of parameters corresponds to $\epsilon \rightarrow 0$.

To study the cosmology of ϕ after reheating we thus consider the following leading terms in its potential

$$V_\phi = m_\phi^2 \phi^2 + \lambda_\phi \frac{\mu_\phi^2}{f^2} \phi^4 \quad (4.3)$$

and treat $\epsilon = m_\phi/\mu_\phi$ as a free parameter. The initial misalignment of the field ultimately arises from the quantum spreading of the field, ϕ , during inflation. If the reheating temperature, T_{RH} , is smaller than the weak scale, i.e. $T_{RH} \lesssim v \sim \sqrt{\mu_\phi f}$, we do not expect any significant thermal corrections to either the 2HDM or the ϕ -potential. At higher temperatures, thermal corrections to the ϕ -potential are model-dependent and depend on the UV origin of the ϕ -field. For the sake of definiteness, we assume here that ϕ is the axion of a strongly coupled sector with a confinement scale given by $M \sim \sqrt{\mu_\phi f} \sim v$. The potential in eq. (4.3) will thus vanish for, $T_{RH} \gtrsim v$, and reappear only when the temperature drops below the weak scale. As the ϕ -potential becomes flat for such high reheating temperatures, we assume that ϕ retains its position in field space during this process. We thus assume that the order of the initial misalignment, $\delta\phi_m$, is given by the amount of quantum spreading of ϕ during inflation.

To study the post-inflationary cosmology of ϕ we must keep in mind two important scales, one of them being the initial misalignment scale, $\delta\phi_m$. The other scale corresponds to the ϕ -field value up to which the quadratic term dominates over the quartic one,

$$\delta\phi_q \sim \epsilon f / \sqrt{\lambda_\phi}. \quad (4.4)$$

The cosmology of ϕ depends on the relative value of these two scales. If $\delta\phi_m \gg \delta\phi_q$, we can ignore the small region where the quadratic term becomes relevant, whereas if, $\delta\phi_m \ll \delta\phi_q$, ϕ only feels the quadratic part of the potential so that we can effectively ignore the quartic and other higher order terms. In App. A we estimate the quantum spreading of ϕ during inflation, and thus the misalignment scale to be,

$$\begin{aligned} \delta\phi_m &\sim \frac{H_I^2}{m_\phi} && (\delta\phi_m \ll \delta\phi_q) \\ \delta\phi_m &\sim \frac{H_I}{\lambda_\phi^{1/4}} \sqrt{\frac{f}{\mu_\phi}} && (\delta\phi_m \gg \delta\phi_q). \end{aligned} \quad (4.5)$$

Using either of the two expressions for $\delta\phi_m$, we can recast the condition to be in the quadratic regime as follows,

$$H_I \lesssim \epsilon \sqrt{\mu_\phi f} / \lambda_\phi^{1/4}, \quad (4.6)$$

where the reverse inequality is required for the quartic regime. We now consider both these regimes.

4.1 Quartic regime

If the Higgs sector parameters are scanned very finely we are in the limit, $\epsilon \ll 1$, so that we can take $\delta\phi_m \gg \delta\phi_q$ and effectively ignore the quadratic term in eq. (4.4). To study the cosmological evolution of, ϕ , after reheating we need to solve its equation of motion,

$$\ddot{\phi} + 3H(T)\dot{\phi} + V'(\phi) = 0 \quad (4.7)$$

where, H , is the Hubble scale, T is the temperature and we take $V(\phi) = \lambda_\phi \frac{\mu_\phi^2}{f^2} \phi^4$. This equation has been studied in detail in Ref. [38, 39]. The above equation admits an oscillatory solution for $H(T) \lesssim \nu$, where ν is the frequency given by,

$$\nu = \frac{4 \Gamma(\frac{3}{4})}{2\sqrt{2\pi}\Gamma(\frac{1}{4})} \left(\frac{\lambda_\phi \mu_\phi^2}{f^2} \rho_\phi \right)^{1/4} \quad (4.8)$$

and ρ_ϕ is the energy density of the ϕ -field.

The oscillations begin at a temperature, $T_{osc} = \min\{v, T_{RH}, T_{sol}\}$, T_{sol} , being the temperature for which, $H(T_{sol}) = \nu$. Once the oscillatory behavior begins, the energy density in the ϕ -field scales as $1/a^4$. Thus the ϕ effectively acts like a source of dark radiation that is constrained to be much smaller than the energy density in the SM sector. If, at the beginning of the oscillations, we require the energy density of ϕ to be much smaller than the expected energy density from standard cosmology, it will remain so throughout cosmological history.⁹ We find that if $T_{osc} = T_{sol}$ or $T_{osc} = v$ this requirement is automatically satisfied, where we have used eq. (2.9) and the fact that the initial value of $\rho_\phi = \lambda_\phi \frac{\mu_\phi^2}{f^2} (\delta\phi_m)^4 \sim H_I^4$ (see eq. (4.5)). If on the other hand, $T_{osc} = v$, we must require $H_I^4 \ll g_\star(T_{RH}) T_{RH}^4$, $g_\star(T_{RH})$ being the number of relativistic degrees of freedom at the reheating temperature.

4.2 Quadratic regime and wave-like dark matter

In the quadratic regime, we take $V_\phi = m_\phi^2 \phi^2/2$ in eq. (4.7). As is well known, this results in damped oscillations of ϕ that can account for dark matter. The dark matter abundance is given by (see for instance [40]),

$$\Omega_\phi h^2 \approx 3 (\Delta\theta_m)^2 \left(\frac{m_\phi}{1 \text{ eV}} \right)^2 \left(\frac{f}{10^9 \text{ GeV}} \right)^2 \left(\frac{100 \text{ GeV}}{T_{osc}} \right)^3. \quad (4.9)$$

where, $T_{osc} \sim \min[v, T_{RH}, T_{sol}]$, is the temperature at which the oscillations begin. Here T_{sol} is determined by solving $3H(T_{sol}) = m_\phi$.

The initial misalignment angle $\Delta\theta = \delta\phi_m/f$, can be varied by changing the inflationary Hubble scale (see eq. (4.5)). Given the requirement in eq. (4.6), we find that the maximal value for the misalignment angle is $\Delta\theta \lesssim \epsilon$, where ϵ itself must satisfy $\epsilon \lesssim 1$. In Fig. 4 we show the ‘dark matter band’, i.e. the region in the m_ϕ - f parameter space where ϕ can explain the dark matter density by adjusting H_I to give an appropriate value of $\Delta\theta$. This is the region between the two solid black lines in Fig. 4. We show the value of $\Delta\theta$ required to obtain the observed dark matter density at the two edges of this band. The region above the band is disallowed in our model because $m_\phi f = \epsilon \mu_\phi f$ cannot exceed v^2 by eq. (2.29).

In the region below the dark matter band, ϕ , can only account for a fraction of the observed dark matter even for a maximal, $\Delta\theta = 1$. This is shown in Fig. 4 by contours of the maximal dark matter density, $[\rho_\phi]_{\max}$. In the presence of the couplings in eq. (4.1),

⁹Here we are assuming that ϵ is small enough such that the ϕ -field value never becomes smaller than $\delta\phi_q$ due to the $1/a$ damping.

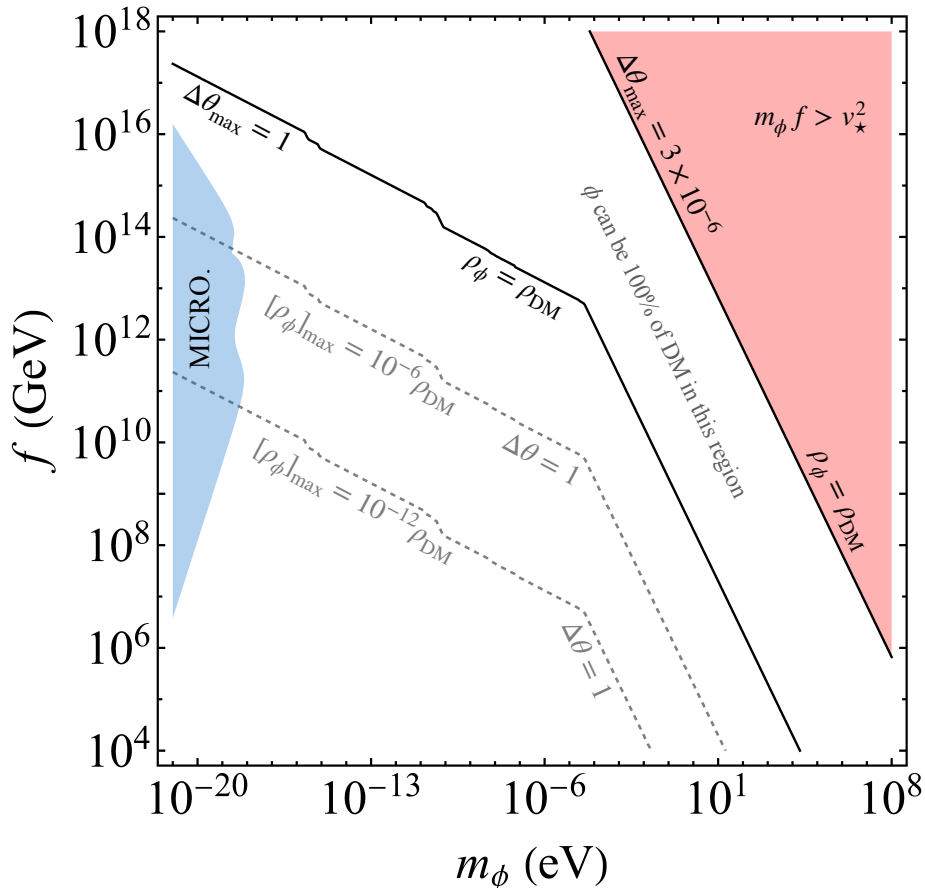


Figure 4: The region in the m_ϕ - f parameter space where the pseudoscalar, ϕ , can account for the observed dark matter of the universe. In the region between the two solid black lines, ϕ can account for all of the observed dark matter by appropriately choosing a misalignment angle, $\Delta\theta \leq 1$. In the region below this band, ϕ alone can constitute only a fraction of the dark matter even if we take the maximal value, $\Delta\theta = 1$ (see dotted contours). The region above this band is excluded in our model because, $m_\phi f > v_\star^2$. In blue we show the bounds from the MICROSCOPE experiment on any apparent violation of the equivalence principle.

the earth can source a spatial dependence of the amplitude of the ϕ -oscillations. This generates an additional force on the test bodies resulting in an apparent violation of the equivalence principle [37, 41]. The strongest bounds on this effect were obtained by the MICROSCOPE experiment [42]; we show the corresponding constraints on our parameter space, assuming positive, $\mathcal{O}(1)$ values for the c_i in eq. (4.1) and conservatively taking the misalignment angle to be at its maximal value, $\Delta\theta = 1$. The oscillations of ϕ would also lead to a time-variation of fundamental constants like the mass of electron and the fine-structure constants. We find, however, that present experiments (see for instance Ref. [43]) do not have the required sensitivity to probe our model mainly because the fraction of dark matter generated is not sufficient in the relevant parts of the parameter space.

5 Conclusions

We have presented a solution to the hierarchy problem up to the scale, $\Lambda \sim \sqrt{vM_{pl}}$. Apart from the inflaton sector, we introduce a light PNBG scalar and an additional Higgs doublet. The main idea of our mechanism has been summarised in Fig. 1 and 2. As shown in Fig. 1, we consider a landscape of vacua across which the Higgs sector parameters, and thus the electroweak VEV, is allowed to vary. By construction, the vacuum energy of the Higgs sector peaks in vacua with an electroweak scale much smaller than the cutoff (see Fig. 2). During eternal inflation this results in patches with maximal vacuum energy—and a hierarchically small electroweak scale—expanding exponentially faster than other patches to eventually dominate the universe in volume. While this maximal energy state can still tunnel into lower vacua, such transitions are exponentially suppressed.

Our model builds on the earlier work of Ref. [5, 6, 8, 11]. As in these works, the key feature of our mechanism is the exponentially higher rate of inflationary expansion of patches where the electroweak VEV is small compared to the cutoff. There is, however, a crucial difference between our model compared to previous ones. In our model, the light field, ϕ , does not scan the Higgs mass and plays a role only in the selection mechanism. We assume instead the presence of a landscape of vacua having different values for low energy parameters and thus different values of the electroweak VEV. It is in this sense that our approach is minimal. While our model may be less ambitious in this regard, the decoupling of the scanning and selection mechanisms, in fact, gives our model a unique simplicity and several advantages. The light field ϕ , in our model, has a completely generic PNBG-like potential with no additional small parameters. In particular, our model does not run into the issues discussed in Ref. [22] and thus does not require an elaborate clockwork sector. The field value of ϕ never exceeds its decay constant and is therefore never transplanckian.

An appealing feature of this work is that, unlike the case of anthropic selection [19], our selection mechanism is robust to the variation of almost all the parameters of our model (the only exception being the sign of the mass term in the ϕ -potential). In particular, we freely vary the quartics of the 2HDM sector and the trigger term. We find that maximizing the vacuum energy with respect to the variation of these parameters automatically selects regions in the landscape with desirable properties—such as electromagnetism remaining unbroken after minimization of the 2HDM.

The maximization of the vacuum energy with respect to the quartics also yields the smoking gun signature of our model, namely the prediction of $\tan\beta$ as a function of other measurable parameters, namely the heavier CP even Higgs mass, m_H and the other mixing angle α (see eq. (3.2)). This is shown in Fig. 3 where we show predictions for $\cos(\beta - \alpha)$ —the parameter that controls the couplings of the SM-like Higgs boson—as a function of the mass of the heavier Higgs, m_H and $\tan\beta$. This is a precise prediction that can be confirmed or falsified by careful measurement of the masses and couplings of the different Higgs bosons of the 2HDM sector. As far as the pseudoscalar in our model is concerned, it can account for the observed dark matter density via the misalignment mechanism in certain regions of the parameter space (see Fig. 4). It can also be probed by experiments looking for a violation of the equivalence principle and future tests of the variation of

fundamental constants.

To summarise we have proposed a simple, non-anthropocentric selection mechanism that explains the smallness of the weak scale and provides smoking gun signatures that can be probed in present and future experiments.

Acknowledgements We are grateful to Sandip Trivedi for insightful discussions and comments that cleared up many of our questions about the landscape. We thank Abhishek Banerjee for patiently explaining to us the MICROSCOPE bounds and Siddhartha Karmakar for discussions during the initial stages of this work. We also thank Ryuichiro Kitano and Avik Banerjee for their comments on this work. We acknowledge the support from the Department of Atomic Energy (DAE), Government of India, under Project Identification Number RTI 4002.

A Quantum Fluctuations and the volume-weighted Fokker-Planck equation

In this appendix, we discuss the role of quantum fluctuations of the scalar fields during inflation. We follow the approach and notation of Ref. [6, 44] closely. We consider first the pseudoscalar field, ϕ . During eternal inflation, ϕ undergoes quantum fluctuations which can be modeled as a random walk with a typical step-size of $\Delta\phi \sim H_I/2\pi$, superimposed on the classical slow-roll trajectory. This results in the evolution of the volume-weighted distribution of ϕ across different Hubble patches, $P(\phi, t)$ according to the volume weighted Fokker-Planck (FPV) equation given by,

$$\frac{\partial P}{\partial t} = \frac{\partial}{\partial \phi} \left[\frac{H_I^3(\phi)}{8\pi^2} \frac{\partial P}{\partial \phi} + \frac{V'(\phi)}{3H_I(\phi)} P \right] + 3H_I(\phi)P. \quad (\text{A.1})$$

Now using eq. (2.29) and eq. (2.30), we see that the value of V_ϕ in eq. (2.1) (or indeed any of the terms of V_H in eq. (2.7)) is a small perturbation on the total vacuum energy during inflation. We thus substitute in eq. (A.1), $P(\phi, t) = \exp(3H_{I_0}t) \exp(-\nu(\phi)) \psi(\phi, t)$, with $\nu(\phi) \equiv 4\pi^2 V(\phi)/3H_{I_0}^4$, to obtain,

$$-\frac{4\pi^2}{H_{I_0}^3} \frac{\partial \psi}{\partial t} = -\frac{1}{2} \frac{\partial^2 \psi}{\partial \phi^2} + \frac{1}{2} \left[-\nu''(\phi) + (\nu'(\phi))^2 - \frac{3}{M_{pl}^2} \nu(\phi) \right] \psi, \quad (\text{A.2})$$

which is the Schrödinger equation with $t \rightarrow it$. Here, H_{I_0} is the Hubble scale corresponding to the vacuum energy with $\phi = 0$. We can make an eigenvalue decomposition of the form $\psi(\phi, t) \equiv \sum_n c_n \psi_n(\phi) e^{-\Gamma_n t}$. The eigenstates ψ_n satisfy the time-independent Schrödinger equation,

$$\frac{4\pi^2 f^2}{H_{I_0}^3} \Gamma_n \psi_n = -\frac{1}{2} \frac{\partial^2 \psi_n}{\partial x^2} + \frac{1}{2} \left[-\nu''(x) + (\nu'(x))^2 - \frac{3f^2}{M_{pl}^2} \nu(x) \right] \psi_n, \quad (\text{A.3})$$

where $x \equiv \phi/f$. After a sufficiently long time, it is expected that $\psi(\phi, t)$ will be dominated by the solution corresponding to the minimum eigenvalue which we call $\psi_0(x)$.

Taking $\nu(x) = \eta \sum_n \lambda_n x^{2n}$, and $\eta \equiv 4\pi^2 \mu_\phi^2 f^2 / 3H_{I_0}^4$ we estimate the different terms in eq. (A.3) to be: $\nu'' \sim \eta$, $(\nu')^2 \sim \eta^2$ and $\frac{3f^2}{M_{pl}^2} \nu(x) \sim \frac{f^2}{M_{pl}^2} \eta$. In the limit $\eta \gg 1$ (which gives the second equation in eq. (2.9)), the dominant contribution to the effective potential within the square brackets comes from the $(\nu')^2$ term which is minimized at the extrema of V_ϕ . Furthermore, assuming $f^2 \ll M_{pl}^2$ (which gives the third equation in eq. (2.9)) we see that the $-\nu''$ term lifts the maxima of V_ϕ so that $\psi(x)$, and thus the volume weighted distribution, peaks at the minima of V_ϕ as expected classically.

A similar analysis can be carried out for the Higgs fields. We can analogously define $\eta_H \equiv 4\pi^2 v^4 / 3H_{I_0}^4$ so that $\eta_H \gg 1$ (which gives the first equation in eq. (2.9)) becomes the limit in which the distribution function of the Higgs fields are peaked around their classical minima.

We now estimate the spread of the distribution of the field, ϕ . This determines the misalignment angle of ϕ . If the dominant contribution to the potential comes from some power p of ϕ , i.e. $\nu(x) \sim \eta x^p$ and $\eta \gg 1$, then it is evident that if $\psi_{0,1}(x)$ is a solution of eq. (A.3) with $\eta = \eta_1$ and $\Gamma = \Gamma_{0,1}$, then $\psi_{0,2}(x) = \psi_{0,1}\left(\left(\frac{\eta_2}{\eta_1}\right)^{\frac{1}{p}} x\right)$ is the solution of eq. (A.3) with $\eta = \eta_2$ and $\Gamma_{0,2} = \Gamma_{0,1}\left(\frac{\eta_2}{\eta_1}\right)^{\frac{2}{p}}$. Thus, the width of ψ_0 must scale as $\eta^{-\frac{1}{p}}$. The width of $P(\phi, t)$ also goes as $\eta^{-\frac{1}{p}}$ because the argument of the exponential $\exp(-\nu(\phi))$ is invariant under such a rescaling. This gives us the misalignment scale given by eq. (4.5). Note that for the quadratic regime discussed in Sec. 4, we must take $\eta_q \equiv 4\pi^2 m_\phi^2 (\delta\phi_q)^2 / 3H_{I_0}^4$ and $\delta\phi_m \sim \delta\phi_q / \eta_q$.

B Minimization of the 2HDM potential

In this appendix, we provide details about the minimization of the 2HDM potential in eq. (2.5) using some of the results of Ref. [28]. The 8 minimization conditions corresponding to the 8 components of the two doublets,

$$H_1 = \frac{1}{\sqrt{2}} \begin{pmatrix} \phi_1 + i\phi_2 \\ \phi_3 + i\phi_4 \end{pmatrix} \quad H_2 = \frac{1}{\sqrt{2}} \begin{pmatrix} \phi_5 + i\phi_6 \\ \phi_7 + i\phi_8 \end{pmatrix}, \quad (\text{B.1})$$

are given by,

$$\phi_1 : \frac{u}{\sqrt{2}} v_1 v_2 \left(\lambda_4 \cos\xi + \hat{\lambda}_5 \cos(\alpha + \xi) \right) = 0 \quad (\text{B.2})$$

$$\phi_2 : \frac{u}{\sqrt{2}} v_1 v_2 \left(-\lambda_4 \sin\xi + \hat{\lambda}_5 \sin(\alpha + \xi) \right) = 0 \quad (\text{B.3})$$

$$\phi_3 : \frac{v_1}{\sqrt{2}} \left(2\lambda_1 v_1^2 + u^2 \lambda_3 + v_2^2 (\lambda_3 + \lambda_4) + 2\mu_1^2 + \hat{\lambda}_5 \cos(\alpha + 2\xi) v_2^2 \right) = 0 \quad (\text{B.4})$$

$$\phi_4 : \frac{v_2^2}{\sqrt{2}} v_1 \hat{\lambda}_5 \sin(\alpha + 2\xi) = 0 \quad (\text{B.5})$$

$$\phi_5 : \frac{u}{\sqrt{2}} \left(2(u^2 + v_2^2) \lambda_2 + v_1^2 \lambda_3 + 2\mu_2^2 \right) = 0 \quad (\text{B.6})$$

$$\phi_6 : 0 \quad (\text{B.7})$$

$$\phi_7 : \frac{v_2}{\sqrt{2}} (2(u^2 + v_2^2)\lambda_2 + v_1^2(\lambda_3 + \lambda_4) + \mu_2^2) \cos\xi + \frac{v_1^2}{\sqrt{2}} v_2 \hat{\lambda}_5 \cos(\alpha + \xi) = 0 \quad (\text{B.8})$$

$$\phi_8 : \frac{v_2}{\sqrt{2}} (2(u^2 + v_2^2)\lambda_2 + v_1^2(\lambda_3 + \lambda_4) + 2\mu_2^2) \sin\xi - \frac{v_1^2}{\sqrt{2}} v_2 \hat{\lambda}_5 \sin(\alpha + \xi) = 0. \quad (\text{B.9})$$

where we have used $SU(2)_L \times U(1)_Y$ invariance to write,

$$\langle H_1 \rangle = \frac{1}{\sqrt{2}} \begin{pmatrix} 0 \\ v_1 \end{pmatrix} \quad \langle H_2 \rangle = \frac{1}{\sqrt{2}} \begin{pmatrix} u \\ v_2 e^{i\xi} \end{pmatrix}. \quad (\text{B.10})$$

From the above equations, it is evident that the VEVs of the two doublets must take the form in eq. (2.22) and eq. (2.23). When $u = 0$ the doublet VEVs are given by eq. (2.22) and minimization with respect to ξ yields two solutions, $\xi = -\alpha/2, -\alpha/2 + \pi$ but only the first one is relevant to us as the second solution does not satisfy the condition in eq. (2.21) as we have chosen $\kappa > 0$. Thus, the potential for this case after substituting eq. (2.22) becomes,

$$V_{2\text{HDM}} = \frac{\mu_1^2 v_1^2}{2} + \frac{\mu_2^2 v_2^2}{2} + \frac{\lambda_1 v_1^4}{4} + \frac{\lambda_2 v_2^4}{4} + \frac{\lambda_{345} v_1^2 v_2^2}{4}, \quad (\text{B.11})$$

where we recall that $\lambda_{345} = \lambda_3 + \lambda_4 + \hat{\lambda}_5$. Minimizing eq. (B.11) with respect to v_1 and v_2 , we obtain

$$\mu_{1,2}^2 = -\lambda_{1,2} v_{1,2}^2 - \frac{\lambda_{345}}{2} v_{2,1}^2, \quad (\text{B.12})$$

which can be used to obtain eq. (2.25). We can also use eq. (B.12) to write v and $\tan\beta$ in terms of the underlying parameters of the potential,

$$v^2 = \frac{4\lambda_2 \mu_1^2 + 4\lambda_1 \mu_2^2 - 2\lambda_{345}(\mu_1^2 + \mu_2^2)}{\lambda_{345} - 4\lambda_1 \lambda_2}$$

$$\tan^2 \beta = \frac{2\lambda_1 \mu_2^2 - \lambda_{345} \mu_1^2}{2\lambda_2 \mu_1^2 - \lambda_{345} \mu_2^2}. \quad (\text{B.13})$$

We now show that class II minima always have smaller vacuum energy than class I minima. For this we consider the potential $\hat{V}_{2\text{HDM}}$ and study its minimisation in the radial direction, $\rho = \sqrt{\sum_{i=1}^8 \phi_i^2}$. First, we use eq. (B.10) to express the two doublets as,

$$\langle H_1 \rangle = \frac{1}{\sqrt{2}} \begin{pmatrix} 0 \\ \rho \cos\beta \end{pmatrix} \quad \langle H_2 \rangle = \frac{1}{\sqrt{2}} \begin{pmatrix} \rho \sin\beta \\ \rho \sin\beta \cos\gamma e^{i\xi} \end{pmatrix}. \quad (\text{B.14})$$

which can be used to write the potential as follows,

$$\hat{V}_{2\text{HDM}} = \frac{\hat{\mu}_\rho^2 \rho^2}{2} + \frac{\hat{\lambda}_\rho \rho^4}{4}. \quad (\text{B.15})$$

where,

$$\hat{\lambda}_\rho \equiv \left(\lambda_1 \cos^4 \beta + \lambda_2 \sin^4 \beta + \frac{\lambda_3}{4} \sin^2 2\beta + \frac{\lambda_4}{4} \sin^2 2\beta \cos^2 \gamma + \frac{\hat{\lambda}_5}{4} \sin^2 2\beta \cos^2 \gamma \cos(\alpha + 2\xi) \right. \\ \left. - \frac{\kappa^2}{16\lambda_\phi} \sin^2 2\beta \cos^2 \gamma \cos^2 \xi \right), \quad (\text{B.16})$$

$$\hat{\mu}_\rho^2 \equiv \left(\mu_1^2 \cos^2 \beta + \mu_2^2 \sin^2 \beta + \frac{\kappa \mu_\phi f}{8\lambda_\phi} \sin 2\beta \cos \gamma \cos \xi \right). \quad (\text{B.17})$$

Using the minimization conditions we get,

$$v^2 = \frac{-\hat{\mu}_\rho^2}{\hat{\lambda}_\rho} \quad (\text{B.18})$$

where the vacuum energy contribution from the 2HDM sector,

$$\mathcal{V}\mathcal{E}_{2HDM} = \frac{-\hat{\mu}_\rho^4}{4\hat{\lambda}_\rho} \quad (\text{B.19})$$

is clearly negative.

Finally, let us show that class I and III minima cannot coexist. We can again recast the ϕ -independent part of the potential in eq. (2.7), V_{2HDM} , to the form given in eq. (B.15), i.e.,

$$V_{2HDM} = \frac{\mu_\rho^2 \rho^2}{2} + \frac{\lambda_\rho \rho^4}{4}. \quad (\text{B.20})$$

where $\{\mu_\rho, \lambda_\rho\} = \{\mu_\rho, \lambda_\rho\}|_{\kappa \rightarrow 0}$. This potential will have an electroweak symmetry breaking minima only if $\mu_\rho^2 < 0$ and $\lambda_\rho^2 > 0$. The first of these conditions can be written as

$$\mu_1^2 c_\beta^2 + \mu_2^2 s_\beta^2 < 0 \quad (\text{B.21})$$

which requires either μ_1^2 or μ_2^2 to be negative. Thus class III minima cannot coexist with class I minima where both μ_1^2 and μ_2^2 must be positive. We can also use eq. (B.20) to write the vacuum energy at the minimum to be $-\lambda_\rho v^4/4$ which again gives eq. (2.25).

References

- [1] G. Dvali and A. Vilenkin, *Cosmic attractors and gauge hierarchy*, *Phys. Rev. D* **70** (2004) 063501 [[hep-th/0304043](#)].
- [2] G. Dvali, *Large hierarchies from attractor vacua*, *Phys. Rev. D* **74** (2006) 025018 [[hep-th/0410286](#)].
- [3] P.W. Graham, D.E. Kaplan and S. Rajendran, *Cosmological Relaxation of the Electroweak Scale*, *Phys. Rev. Lett.* **115** (2015) 221801 [[1504.07551](#)].
- [4] N. Arkani-Hamed, T. Cohen, R.T. D’Agnolo, A. Hook, H.D. Kim and D. Pinner, *Solving the Hierarchy Problem at Reheating with a Large Number of Degrees of Freedom*, *Phys. Rev. Lett.* **117** (2016) 251801 [[1607.06821](#)].
- [5] M. Geller, Y. Hochberg and E. Kuflik, *Inflating to the Weak Scale*, *Phys. Rev. Lett.* **122** (2019) 191802 [[1809.07338](#)].
- [6] C. Cheung and P. Saraswat, *Mass Hierarchy and Vacuum Energy*, [1811.12390](#).
- [7] G.F. Giudice, A. Kehagias and A. Riotto, *The Selfish Higgs*, *JHEP* **10** (2019) 199 [[1907.05370](#)].
- [8] A. Strumia and D. Teresi, *Relaxing the Higgs mass and its vacuum energy by living at the top of the potential*, *Phys. Rev. D* **101** (2020) 115002 [[2002.02463](#)].
- [9] C. Csáki, R.T. D’Agnolo, M. Geller and A. Ismail, *Crunching Dilaton, Hidden Naturalness*, *Phys. Rev. Lett.* **126** (2021) 091801 [[2007.14396](#)].

- [10] N. Arkani-Hamed, R.T. D’Agnolo and H.D. Kim, *Weak scale as a trigger*, *Phys. Rev. D* **104** (2021) 095014 [2012.04652].
- [11] G.F. Giudice, M. McCullough and T. You, *Self-organised localisation*, *JHEP* **10** (2021) 093 [2105.08617].
- [12] R. Tito D’Agnolo and D. Teresi, *Sliding Naturalness: New Solution to the Strong-CP and Electroweak-Hierarchy Problems*, *Phys. Rev. Lett.* **128** (2022) 021803 [2106.04591].
- [13] R. Tito D’Agnolo and D. Teresi, *Sliding naturalness: cosmological selection of the weak scale*, *JHEP* **02** (2022) 023 [2109.13249].
- [14] C. Csaki, A. Ismail, M. Ruhdorfer and J. Tooby-Smith, *Higgs squared*, *JHEP* **04** (2023) 082 [2210.02456].
- [15] O. Matsedonskyi, *Hierarchies from Landscape Probability Gradients and Critical Boundaries*, [2311.10139](#).
- [16] P. Bak, C. Tang and K. Wiesenfeld, *Self-organized criticality: An explanation of the 1/f noise*, *Phys. Rev. Lett.* **59** (1987) 381.
- [17] G.F. Giudice, *Naturally Speaking: The Naturalness Criterion and Physics at the LHC*, [0801.2562](#).
- [18] S. Weinberg, *Anthropic Bound on the Cosmological Constant*, *Phys. Rev. Lett.* **59** (1987) 2607.
- [19] V. Agrawal, S.M. Barr, J.F. Donoghue and D. Seckel, *Viable range of the mass scale of the standard model*, *Phys. Rev. D* **57** (1998) 5480 [[hep-ph/9707380](#)].
- [20] A.H. Guth, *Eternal inflation and its implications*, *J. Phys. A* **40** (2007) 6811 [[hep-th/0702178](#)].
- [21] J.R. Espinosa, C. Grojean, G. Panico, A. Pomarol, O. Pujolàs and G. Servant, *Cosmological Higgs-Axion Interplay for a Naturally Small Electroweak Scale*, *Phys. Rev. Lett.* **115** (2015) 251803 [1506.09217].
- [22] R.S. Gupta, Z. Komargodski, G. Perez and L. Ubaldi, *Is the Relaxion an Axion?*, *JHEP* **02** (2016) 166 [1509.00047].
- [23] O. Davidi, R.S. Gupta, G. Perez, D. Redigolo and A. Shalit, *The hierarchion, a relaxion addressing the Standard Model’s hierarchies*, *JHEP* **08** (2018) 153 [1806.08791].
- [24] R.S. Gupta, J.Y. Reiness and M. Spannowsky, *All-in-one relaxion: A unified solution to five particle-physics puzzles*, *Phys. Rev. D* **100** (2019) 055003 [1902.08633].
- [25] S. Kachru, R. Kallosh, A.D. Linde and S.P. Trivedi, *De Sitter vacua in string theory*, *Phys. Rev. D* **68** (2003) 046005 [[hep-th/0301240](#)].
- [26] S. Kachru, R. Kallosh, A.D. Linde, J.M. Maldacena, L.P. McAllister and S.P. Trivedi, *Towards inflation in string theory*, *JCAP* **10** (2003) 013 [[hep-th/0308055](#)].
- [27] L. Susskind, *The Anthropic landscape of string theory*, [hep-th/0302219](#).
- [28] J.L. Diaz-Cruz and A. Mendez, *Vacuum alignment in multiscalar models*, *Nucl. Phys. B* **380** (1992) 39.
- [29] A.D. Linde, *Towards a gauge invariant volume-weighted probability measure for eternal inflation*, *JCAP* **06** (2007) 017 [0705.1160].

- [30] M.R. Douglas and S. Kachru, *Flux compactification*, *Rev. Mod. Phys.* **79** (2007) 733 [[hep-th/0610102](#)].
- [31] M. Tegmark, *What does inflation really predict?*, *JCAP* **04** (2005) 001 [[astro-ph/0410281](#)].
- [32] A.D. Linde, V. Vanchurin and S. Winitzki, *Stationary Measure in the Multiverse*, *JCAP* **01** (2009) 031 [[0812.0005](#)].
- [33] A. Linde and M. Noorbala, *Measure Problem for Eternal and Non-Eternal Inflation*, *JCAP* **09** (2010) 008 [[1006.2170](#)].
- [34] A. Arbey, F. Mahmoudi, O. Stal and T. Stefaniak, *Status of the Charged Higgs Boson in Two Higgs Doublet Models*, *Eur. Phys. J. C* **78** (2018) 182 [[1706.07414](#)].
- [35] O. Atkinson, M. Black, A. Lenz, A. Rusov and J. Wynne, *Cornering the Two Higgs Doublet Model Type II*, *JHEP* **04** (2022) 172 [[2107.05650](#)].
- [36] O. Atkinson, M. Black, C. Englert, A. Lenz, A. Rusov and J. Wynne, *The flavourful present and future of 2HDMs at the collider energy frontier*, *JHEP* **11** (2022) 139 [[2202.08807](#)].
- [37] A. Banerjee, G. Perez, M. Safronova, I. Savoray and A. Shalit, *The phenomenology of quadratically coupled ultra light dark matter*, *JHEP* **10** (2023) 042 [[2211.05174](#)].
- [38] M.S. Turner, *Coherent Scalar Field Oscillations in an Expanding Universe*, *Phys. Rev. D* **28** (1983) 1243.
- [39] E. Masso, F. Rota and G. Zsembinszki, *Scalar field oscillations contributing to dark energy*, *Phys. Rev. D* **72** (2005) 084007 [[astro-ph/0501381](#)].
- [40] E.W. Kolb and M.S. Turner, *The Early Universe*, vol. 69, Taylor and Francis (5, 2019), [10.1201/9780429492860](#).
- [41] A. Hees, O. Minazzoli, E. Savalle, Y.V. Stadnik and P. Wolf, *Violation of the equivalence principle from light scalar dark matter*, *Phys. Rev. D* **98** (2018) 064051 [[1807.04512](#)].
- [42] MICROSCOPE collaboration, *MICROSCOPE Mission: Final Results of the Test of the Equivalence Principle*, *Phys. Rev. Lett.* **129** (2022) 121102 [[2209.15487](#)].
- [43] R.S. Gupta, J. Jaeckel and M. Spannowsky, *Probing Poincaré violation*, *JHEP* **11** (2023) 026 [[2211.04490](#)].
- [44] P.W. Graham and A. Scherlis, *Stochastic axion scenario*, *Phys. Rev. D* **98** (2018) 035017.